Journal of Mining and Earth Sciences

Website: https://jmes.humg.edu.vn

Active faulting in north-central Vietnam illuminated by fluvial geomorphic analysis: A case study of the Quang Nam basin

Dao Anh Vu *, Hai Thanh Tran, Binh Van Phan, Hau Vinh Bui, Chi Kim Thi Ngo, Hung Quoc Nguyen

Hanoi University of Mining and Geology, Hanoi, Vietnam

ARTICLE INFO

Article history:
Received 06th May 2026
Revised 12th July 2026
Accepted 21st July 2026

Keywords:
Active fault,
Drainage basin asymmetry,
Normalised steepness index,
River longitudinal profile,
Tectonic geomorphology,
Valley floor width to height ratio.

ABSTRACT

North-central Vietnam, including the densely populated Quang Nam basin and the Da Nang - Hoi An urban corridor, has recently experienced earthquakes and associated geohazards such as landslides and coastal erosion, yet neotectonic deformation in the region remains poorly understood. This study integrates field structural observations with newly extracted fluvial geomorphic indices to characterise deformation patterns and potential active faulting in the Quang Nam basin. A 12.5 m ALOS Digital Elevation Model was processed to derive channel and basin metrics, including drainage basin asymmetry, the valley floor width-to-height ratio, the normalised channel steepness index, and knickpoints extracted from modelled longitudinal profiles of 40 rivers. Several knickpoints coincide with lithological boundaries of contrasting erodibility and with artificial dams, whereas many others align along the strike of major faults and are interpreted as having a tectonic origin. Channels intersecting the NE-SW to E-W fault system display anomalously high steepness values; field slickenside indicators on recent fault scarps reveal these structures to be active normal faults. The drainage basin asymmetry of the Quang Nam basin (AF = 60.1) indicates northward tilting of the basin floor, while lower valley floor width-to-height ratios on the northern flank (0.11÷0.61) relative to the southern flank (0.40÷3.72) suggest a higher subsidence rate to the north. Four reactivated structures - the Nam O-Nam Dong, Prao, Kon River and Tam Ky-Phuoc Son faults - are inferred to be active. The results provide geomorphic and field evidence for a distribution of active faults that may pose a seismic and subsidence hazard to the Quang Nam region, with important implications for hazard assessment under rising sea levels. This is the first basin-scale assessment to integrate fluvial geomorphic indices (ksn, AF and Vf) with field kinematic observations across the entire Quang Nam basin: channels crossing the active NE-SW to E-W faults show ksn rising from about 150 to nearly 300 within uniform lithology, providing the principal quantitative evidence for active faulting.

*Corresponding author
E - mail: vuanhdao@humg.edu.vn
DOI: 10.46326/JMES.2026.67(4).08

1. Introduction

Central Vietnam extends for more than 1,000 km along several coastal provinces and major urban centres and is an important socio-economic region of Vietnam. The area lies within the Indochina block, which has been regarded as tectonically active throughout the Cenozoic as a consequence of the India-Eurasia collision (Faure et al., 2014; Sone & Metcalfe, 2008). These activities have driven movement on associated faults, such as the Red River-Ailao Shan fault in the north and the Tra Bong and Tam Ky-Phuoc Son faults in central Vietnam (Hutchison, 1989; Lepvrier et al., 1997; Tri & Khuc, 2011). Although central Vietnam lies far from a plate boundary and is less active than the north, earthquakes occur relatively frequently and may be directly caused by active faults; seismic catalogues report about 30 events since 1980 (International Seismological Centre). In recent years, coastline erosion and beach loss have been reported across the area, threatening the populous cities of Da Nang and Hoi An. Identifying currently active faults and related geohazards is therefore essential for assessing the vulnerability of central Vietnam.

Previous studies have applied geophysical techniques, growth-strata analysis and radiocarbon dating to investigate active tectonics in this area, allowing characterisation of the timing and recurrence interval of specific fault segments (e.g., the Tra Bong fault). However, the long-term history of fault movement is difficult to constrain from instrumental or historical records alone, and there has been little holistic research on the neotectonic deformation of central Vietnam, especially from a tectonic-geomorphology perspective. Morphotectonic analysis can provide valuable information on fault activity through geomorphic indices and topographic evidence (Burbank & Anderson, 2011; Dinh et al., 2021; Whipple et al., 2007; Wobus et al., 2006).

To understand the regional active tectonics, this work integrates existing structural data with new, detailed geomorphic analyses of the fluvial network to characterise potential active vertical deformation in central Vietnam. Because present-day topography commonly conceals the signature of tectonic activity, high-resolution morphological data such as the ALOS DEM are required to extract quantitative geomorphic indices and overcome local surface disturbance (Mukherjee & Joshi, 2013; Santillan & Makinano-Santillan, 2016). River channels are sensitive recorders of base-level change driven by rock uplift or subsidence (Burbank & Anderson, 2011; Whipple, 2004); hence the channel steepness index is particularly insightful for identifying and characterising active structures. Field investigations were conducted to support the DEM-based interpretation, especially the location and kinematics of lineaments and fault systems. The results provide evidence for identifying potential active structures, which is valuable for assessing regional tectonic subsidence and associated flooding hazards under current sea-level-rise scenarios, and for the planning of infrastructure and energy projects in the region. Previous neotectonic studies in central Vietnam have largely targeted individual fault zones; no basin-scale assessment integrating fluvial geomorphic indices with field kinematics has yet been undertaken for the Quang Nam basin, which is the gap addressed here.

2. Regional geological and tectonic setting

2.1. Geological framework

North-central Vietnam, including the Quang Nam basin, is one of the most distinctive crustal domains in Vietnam, forming a transition zone between the Kontum Massif to the south and the Truong Son Belt to the north (Figure 1). The basement juxtaposes high-grade metamorphic rocks of the north-eastern margin of the Kontum Massif against the lower-grade metamorphic rocks of the Truong Son Fold Belt. The rocks comprise mainly Palaeozoic to Cenozoic sedimentary and volcanic sequences intruded by a large volume of Middle Palaeozoic to Early Cenozoic magma and crosscut by scattered mylonitic zones tens to hundreds of kilometres long (Lan et al., 2003; Lepvrier et al., 2004). The oldest units are Cambrian-Ordovician metasedimentary rocks; Cenozoic units include thin Neogene-Quaternary organic-rich layers distributed in small, narrow basins and discontinuous coastal terraces. In this study, the term Quang Nam basin denotes the Cenozoic sedimentary basin occupying the coastal lowland and the lower reaches of the Vu Gia-Thu Bon river system in the Quang Nam-Da Nang region, delimited by the fault systems described below (Figure 2).

For the purpose of assessing rock resistance to weathering and erosion, two main groups are distinguished.

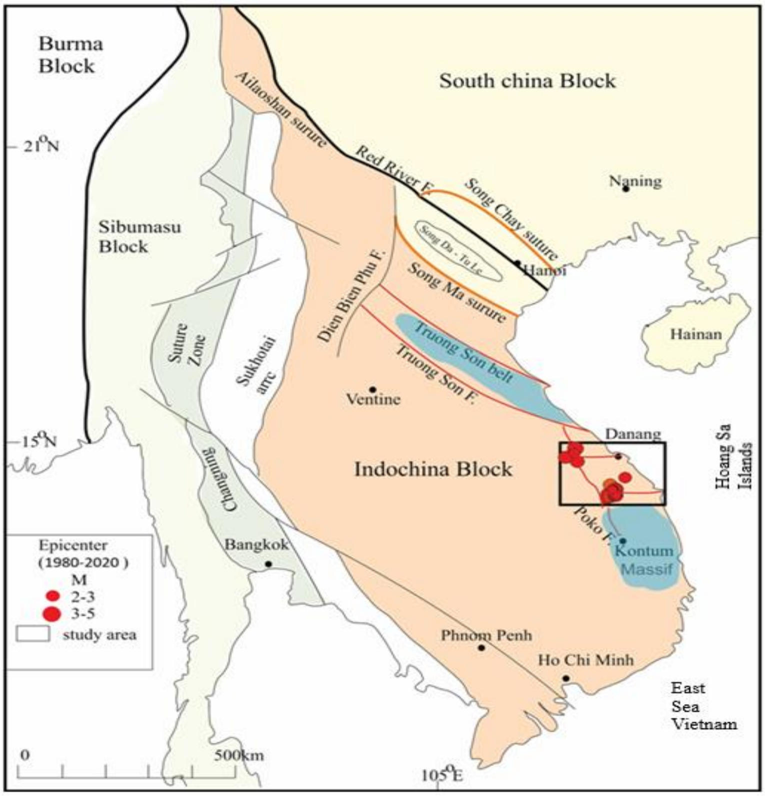

Figure 1. Simplified tectonic and seismicity map (1980-2020) of the Indochina block showing the main faults and the location of the study area (after Lepvrier et al., 2004; Tran et al., 2013).

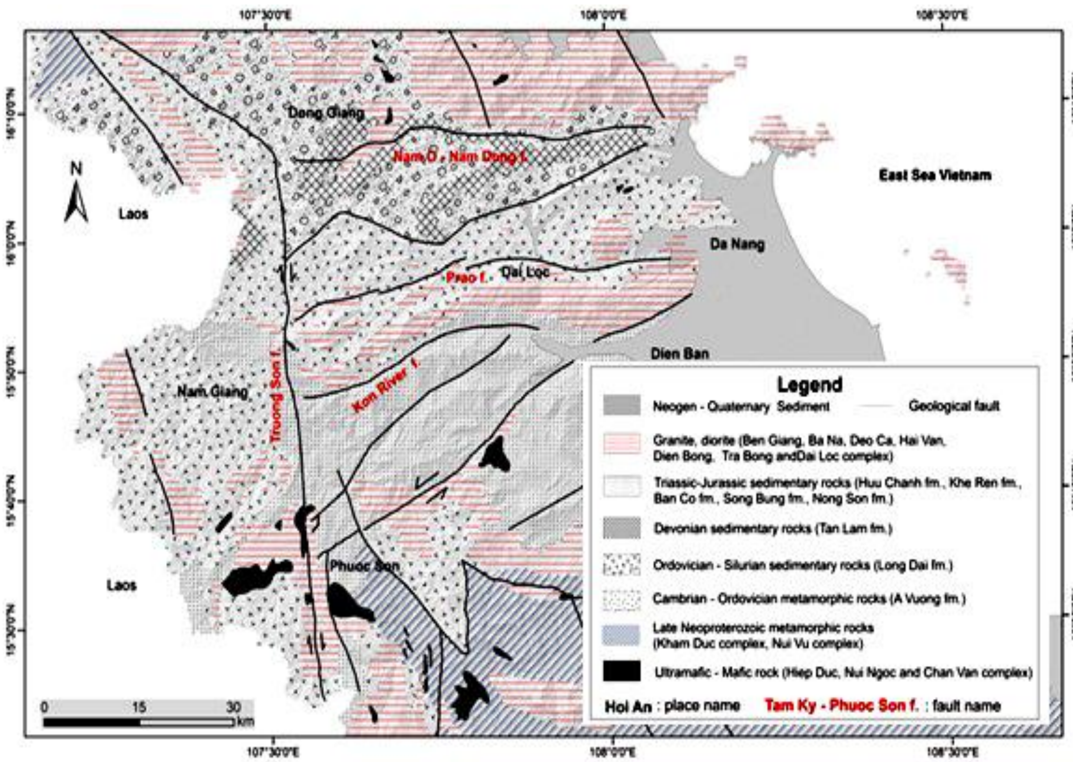

Figure 2. Geological map of the study area (after Nguyen, 1986).

The **sedimentary and metasedimentary** group includes the oldest Kham Duc and Nui Vu formations (hornblende-biotite gneiss, epidote amphibolite and mica schist; detrital zircon age 558±7 Ma; Usuki et al., 2009), the A Vuong, Long Dai, Tan Lam, Huu Chanh, Khe Ren and Ban Co formations, and Quaternary unconsolidated sediments along the narrow Quang Nam coastal plain. The **intrusive** group is represented by the granitoids of the Hai Van, Ben Giang-Que Son, Dai Loc, Ba Na, Deo Ca and Tra Bong complexes, with subordinate altered mafic-ultramafic bodies of the Hiep Duc and Nui Ngoc complexes. Granitoids aged 410÷430 Ma and 250÷240 Ma are widely distributed along the northern margin of the area (Hieu et al., 2016). Intrusive rocks are highly resistant to erosion, whereas the siliciclastic and carbonate successions are on average poorly resistant; these erodibility contrasts must be accounted for when interpreting fluvial geomorphic indices.

2.2. Regional structure

Central Vietnam and the adjacent parts of Indochina record two major tectonic events: the Permo-Triassic Indosinian Orogeny, interpreted as the amalgamation of the Indochina and South China blocks (Lepvrier et al., 2004), and Cenozoic deformation controlled by the indentation of India into Eurasia (Huchon et al., 1994; Tapponnier et al., 1982). The regional structural pattern is inherited from Early-Middle Triassic NW-SE to E-W ductile shear zones and pre-Cenozoic fault zones, such as the Truong Son and Tam Ky-Phuoc Son faults, which were reactivated in response to the India-Eurasia collision. Regional mapping recognises four main fault systems, dominantly NE-SW to sub-latitudinal and less commonly sub-longitudinal and NW-SE (Nguyen, 1986; Tran et al., 2013), including the Truong Son, Tam Ky-Phuoc Son, Nam O-Nam Dong, Prao, Thanh River and Kon River fault zones (Table 1).

Paleostress analysis from the Oligocene to the late Miocene has identified four successive paleostress regimes affecting central Vietnam, reflecting the changing influence of the India-Eurasia collision and the potential for reactivation of ancient faults (Li et al., 2017; Vuong & Hoai, 2019). This study aims to provide further insight into the recent tectonic evolution of central Vietnam.

3. Data and research methods

Topographic analysis and river-profile analysis were combined to detect active tectonic features. Regional topography was examined with swath profiles across the candidate faults of Section 2.2 to identify offset topographic features indicative of recent fault movement (Pérez-Peña et al., 2017). Geomorphic indices were then extracted to detect transient vertical land movement related to neotectonics (Burbank & Anderson, 2011; Keller & Pinter, 2002; Wobus et al., 2006), and the results were combined with field observations to confirm the presence and nature of active structures.

Table 1. Main faults in the study area (after Nguyen, 1986; Tran et al., 2013).

Main fault	Localities	Length (km)	Lithologies of both fault walls	Recent shear sense
Nam O-Nam Dong	From north of Da Nang city (E) to Dong Giang area (W)	60	Devonian sedimentary rocks (Tan Lam Fm.)	Dextral-normal
Prao	From northern Dai Loc (E) to Tay Giang (W)	63	Cambrian-Ordovician metamorphic rocks (A Vuong Fm.)	Normal
Kon River	From Dien Ban (E) to the western area	39	Triassic sedimentary rocks (Nong Son Fm.)	Normal
Tam Ky-Phuoc Son	From Hoi An (E) to Phuoc Son area (W)	100	Late Proterozoic metamorphic rocks (Kham Duc complex)	Normal
Truong Son	Extending southward from west of Kham Duc	100	Cambrian-Triassic (meta)sedimentary rocks	Dextral and sinistral

3.1. Topographic analysis

A 12.5-m DEM from ALOS imagery (Alaska Satellite Facility) was used as the quantitative basis for interpreting deformation in degraded surfaces. Swath profiles - the stacking of many parallel single profiles along a baseline - were extracted using a sampling step of 1.5 times the DEM cell size, with 50 parallel lines per baseline. Low local relief and converging swath lines characterise stable basins or plateaus, whereas high relief and wide swath variation characterise mountain ranges undergoing high incision or uplift (Pérez-Peña et al., 2017). Possible fault lineaments were mapped from the DEM and three-dimensional terrain views in ArcScene 10.3, using geomorphic criteria such as aligned ridges or valleys, anomalously straight coastlines and rivers, aligned lakes and sag ponds, and sharp boundaries between terrain types. Google and SPOT5 imagery were used to cross-check artefacts, and field surveys verified whether mapped features are genuine faults. The vertical accuracy of the 12.5-m ALOS DEM (of the order of a few metres) limits the detection of low-relief knickpoints; this uncertainty was taken into account when interpreting subtle profile breaks.

3.2. River longitudinal profile analysis

River profiles were analysed for channels trending perpendicular to the mapped lineaments. Undisturbed mature streams have a smooth, concave-up profile; perturbations produce convex reaches, or knickpoints, where channels cross faults, lithological boundaries or anthropogenic structures (Di Naccio et al., 2013; Leeder & Jackson, 1993). Knickpoints can reflect base-level lowering, differential erosion, sediment input or man-made obstructions; where tectonic, normal faulting produces a knickpoint through hanging-wall downthrow. The river network was delineated from the filled DEM (flow direction and accumulation, threshold 0.1 km^2) in ArcGIS 10.3 and processed with the StreamProfiler MATLAB tools of Whipple, Wobus and Kirby. The steepness index relates channel slope to drainage area through a power law:

$$S = k_S A^{-\theta} \qquad (1)$$

Where S is the channel slope, A is the upstream drainage area, θ is the concavity index and k_S is the steepness index. To compare channels in different settings, the steepness index is normalised to a reference concavity θ_{ref} = 0.45, yielding the normalised steepness index k_{sn}. Slope-area data, computed within a 3×3 moving window, were plotted in log-log space; a critical drainage area A_c of about 1 km^2 marks the fluvial channel head. Vertical-step knickpoints (anchored to substrate changes or debris flows) generally lack direct tectonic significance, whereas slope-break knickpoints record changes in the forcing of the fluvial system and provide an opportunity to interpret tectonics in erosional landscapes (Kirby & Whipple, 2012; Kirby & Ouimet, 2011; Whipple et al., 2007). The reference concavity θref = 0.45 is the widely adopted regional value that allows steepness to be compared between catchments of different size (Wobus et al., 2006; Kirby & Whipple, 2012). The 40 channels analysed were selected as the trunk rivers that cross or parallel the mapped fault zones and have sufficient length and relief for reliable profile modelling, sampling both flanks of the basin. Knickpoints coinciding with mapped lithological contacts were classed as lithological, those coinciding with dams confirmed on imagery as anthropogenic, and slope-break knickpoints within uniform lithology aligned along mapped faults as tectonic.

3.3. Drainage basin asymmetry analysis

Drainage basin asymmetry (AF) reflects lithological contrast or asymmetric tectonic tilting between the two halves of a basin (Keller & Pinter, 2002):

$$AF = (A_r/A_T) \times 100 \qquad (2)$$

Where A_r is the basin area to the right of the trunk flow direction and A_T is the total basin area. Values near 50 indicate a symmetric, untilted basin; values significantly above 55 or below 45 indicate tectonic or erodibility-driven tilting (Mahmood & Gloaguen, 2012; Ozkaymak & Sozbilir, 2012).

3.4. Valley floor width-to-height ratio analysis

The valley floor width-to-height ratio (Vf) discriminates between actively incising and degrading valleys (Bull & McFadden, 1977; Keller & Pinter, 2002):

$$Vf = 2V_{fw}/[(E_{ld} - E_{sc}) + (E_{rd} - E_{sc})] \qquad (3)$$

Where V_{fw} is the valley floor width, E_{ld} and E_{rd} are the elevations of the left and right divides, and E_{sc} is the elevation of the valley floor. Low Vf values (< 0.5) indicate steeply incised, V-shaped valleys associated with active uplift, whereas values near or above 1.0 indicate broad, U-shaped valleys dominated by widening. Measurements were taken about 5 km up-valley from the range front; because lithology and stream size also influence Vf, the index is treated as a qualitative guide (Pérez-Peña et al., 2010).

3.5. Field investigation

Fieldwork was carried out around the Da Nang-Hoi An area and in rock quarries and mines with outcrops location in Figure 3. Slickenside striations on fault planes were used to determine shear sense and constrain fault kinematics, and prominent fault traces preserved in the landform were sought as geomorphic evidence of recent movement.

4. Results

4.1. Topography and lineament systems

The Quang Nam area comprises low mountainous terrain in the west and a narrow coastal plain in the east, where Da Nang and Hoi An are located. Four lineament systems were recognised: NE-SW and E-W systems are pervasive across the area, whereas sub-longitudinal and NW-SE systems are less common in the south and west (Figure 3). In the west, mountain ranges trend dominantly NE-SW with sharp linear slopes that follow the mapped faults and lithological boundaries. In the Que Hiep, Dai Loc and Duy Xuyen areas, aligned sag ponds and lakes observed on SPOT5 imagery lie along straight lineaments that separate contrasting terrains.

The four swath profiles show contrasting forms: profiles A1 and A2 (left flank of the basin) display wide variation and three southward step-down terrains bounded by the high-angle Prao and Kon River normal faults, whereas profiles B and C show converging lines and weak incision.

4.2. River longitudinal profiles and steepness index

Longitudinal profiles were extracted for 40 rivers - the Quang Nam basin (R1-R22), the southern Hue basin (H1-H15) and the northern Quang Ngai basin (Q1-Q3) (Table 2). In the southern Hue basin, knickpoints on H1-H5 coincide with lithological changes, and the H5 knickpoint

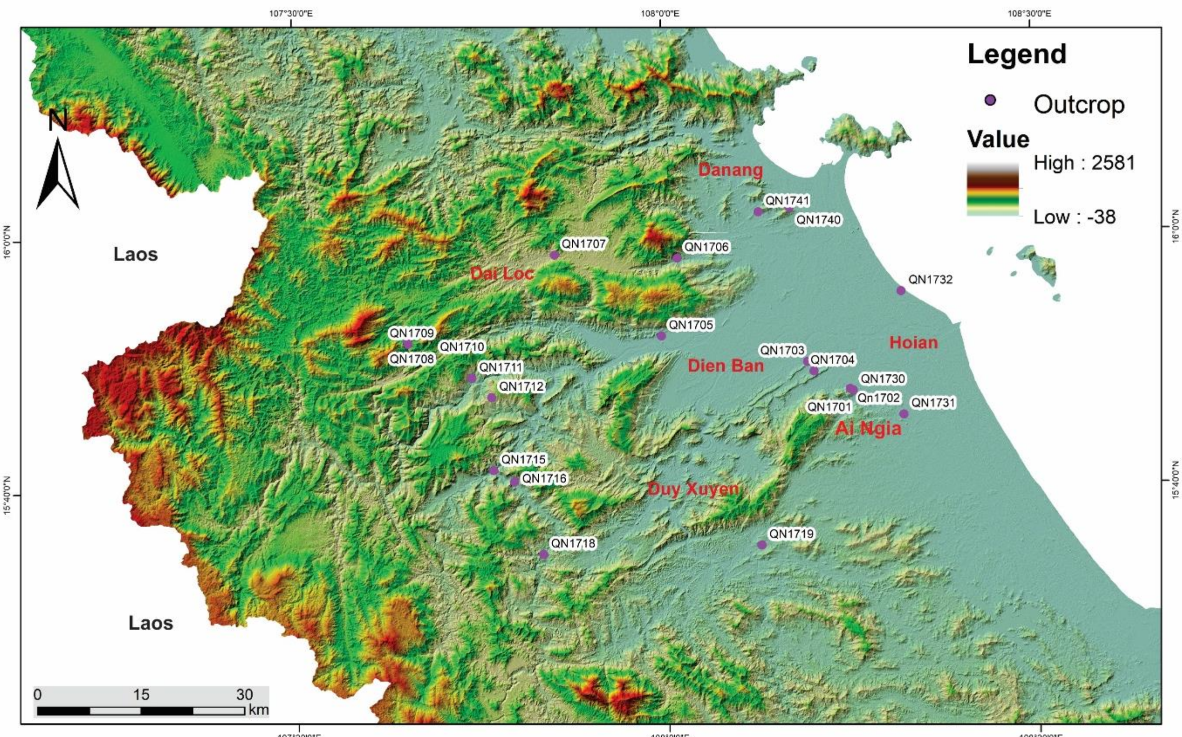

Figure 3. Digital elevation model of the study area showing the distribution of outcrop of field investigation.

Table 2. Normalised steepness index (ksn) of 40 rivers in the study area, listed for distinct channel segments from upstream to downstream. River codes: H - southern Hue basin; R - Quang Nam basin; Q - northern Quang Ngai basin.

River	Abbrev.	L (km)	Segment ksn (up → down)	River	Abbrev.	L (km)	Segment ksn (up → down)
A Luoi	H1	43	103/6.97	Bung	R6	189	151.7/131.7/132.7/65
A Luoi 2	H2	33	125.2/26.9	Tay Giang	R7	160	156.5/135.5/61.2
Huu Trach	H3	24	131/26.4	A Xan	R8	220	153.3/150.1/90.1/56.5
Bo	H4	16	38.6	H Ruh	R9	205	178.3/155.8/139/63.4
Hong Thuong	H5	38	144.8/ 126.1/26.9	Cho Chun	R10	175	195.9/148.8/63.4
Hong Bac	H6	47	162/24.8	Nam Giang	R11	165	170.5/106.5/20.5
Rao Nai	H7	48	142/33.4	Ta Un	R12	165	182.3/149/39
Hong Kim	H8	50	138.7/26.4	Thanh	R13	155	259.6/163/27.5
Huong Hoa	H9	45	127.1/17.3	Dak Mi	R14	155	158/106/29.1
Ta Trach	H10	50	120.4/27.7	Que Lam	R15	90	155.5/115.5/16.4
Thuong Lo	H11	52	181/ 81/18.1	Dak Mi 2	R16	38	156.8/120.2/110.6
Song Bac	H12	35	131/10.4	Thu Bon	R17	52	182.2/113.1/101.1/13.1
Cu De	H13	17	68.6/ 30.2/35.5	Tien Phuoc	R18	65	118.7/110.9/100.9/6.26
Hoa Trung	H14	19	108.5/15	Ly Ly	R19	83	114/7.27
Han	H15	36	107/27.3	Que Hiep	R20	47	108.1/5.65
Za Hung	R1	170	152.7 / 108.9/92.4	Dinh Thi	R21	37	107.1/73.4
Kon	R2	110	150.5 / 295/10.9	Tra Ly	R22	38	100.9/16.29
An Diem	R3	100	151.5/ 293/26	Tam Ky	Q1	48	3.92
Dai Loc	R4	65	306/13	Truong Giang	Q2	35	100.1/4.27
Vu Gia	R5	98	112.6/8.38	Tam Lanh	Q3	17	57.2

coincides with a hydropower dam confirmed on satellite imagery (cf. Figure 4); four slope-break knickpoints on H9, H10, H12 and H13 fall along the Nam O-Nam Dong fault. In the northern Quang Nam basin, segments of R1-R5 crossing the E-W Kon River and Prao faults show an upstream k_{sn} of about 150 increasing to nearly 300 in the middle reach within uniform Triassic Nong Son sediments.

Further west, knickpoints on R8-R15 are mostly vertical-step types coinciding with erodibility contrasts (e.g., the boundary between Ben Giang granite and A Vuong shale) and, locally, with hydropower dams (Figure 4). In the south, high k_{sn} values and knickpoints on R16-R18 (Tien Phuoc River) fall along the Tam Ky-Phuoc Son fault within uniform lithology. By contrast, the R19-R22 rivers (Duy Xuyen area) and the Q1-Q3 rivers of the northern Quang Ngai basin show knickpoints that coincide with lithological boundaries. Spatial interpolation of k_{sn} (Figure 5) delineates high-value zones (> 150) along the NW-SE to E-W structures on both flanks of the basin.

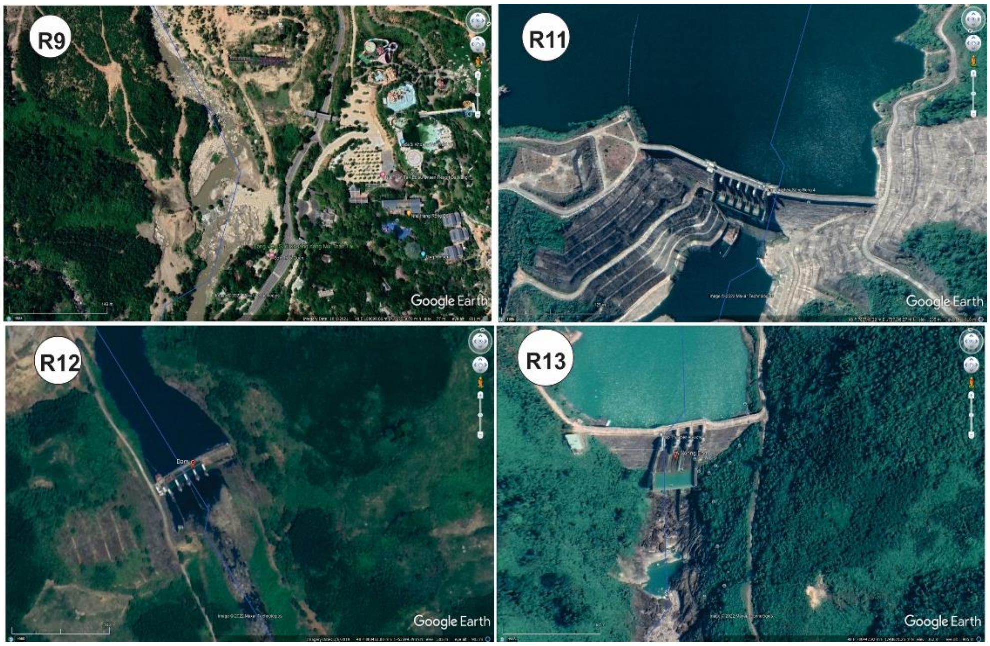

Figure 4. Examples of artificial (dam-induced) knickpoints on the R9, R11, R12 and R13 river profiles, confirmed on Google Earth imagery.

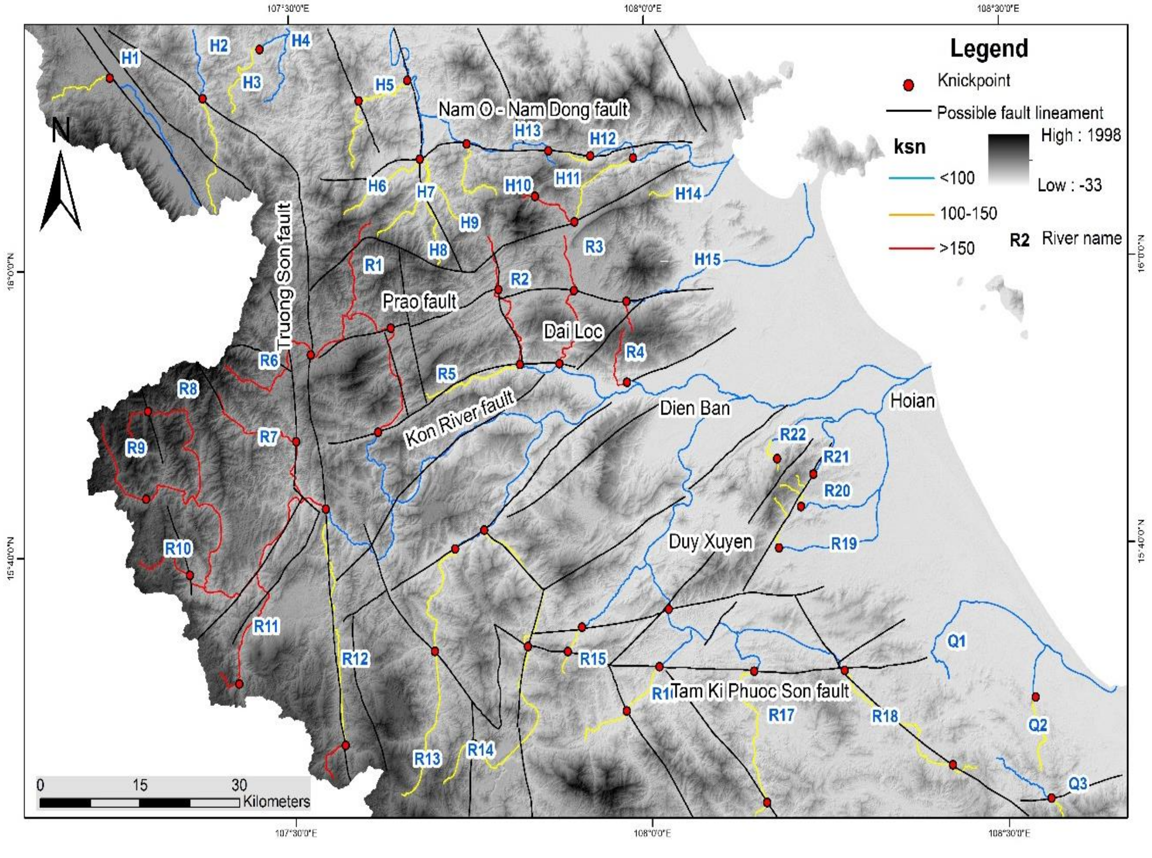

Figure 5. Map of the normalised steepness index (ksn) and the location of knickpoints along the rivers; colours denote different ksn ranges.

4.3. Drainage basin asymmetry

The Quang Nam basin yields AF = 60.1, classifying it as moderately asymmetric, with the basin midline displaced northward (Figure 6).

4.4. Valley floor width-to-height ratio

Vf was measured across valleys crossing the Kon River, Prao, Thanh River and Tam Ky-Phuoc Son faults (Table 3). Values range from 0.11 to 3.72, with predominantly V-shaped valleys and subordinate U-shaped valleys. The northern flank (Vf= 0.11-0.61) yields systematically lower values than the southern flank (Vf = 0.40-3.72) (Figure 7), and the lowest Vf values occur along the Kon River and Prao faults.

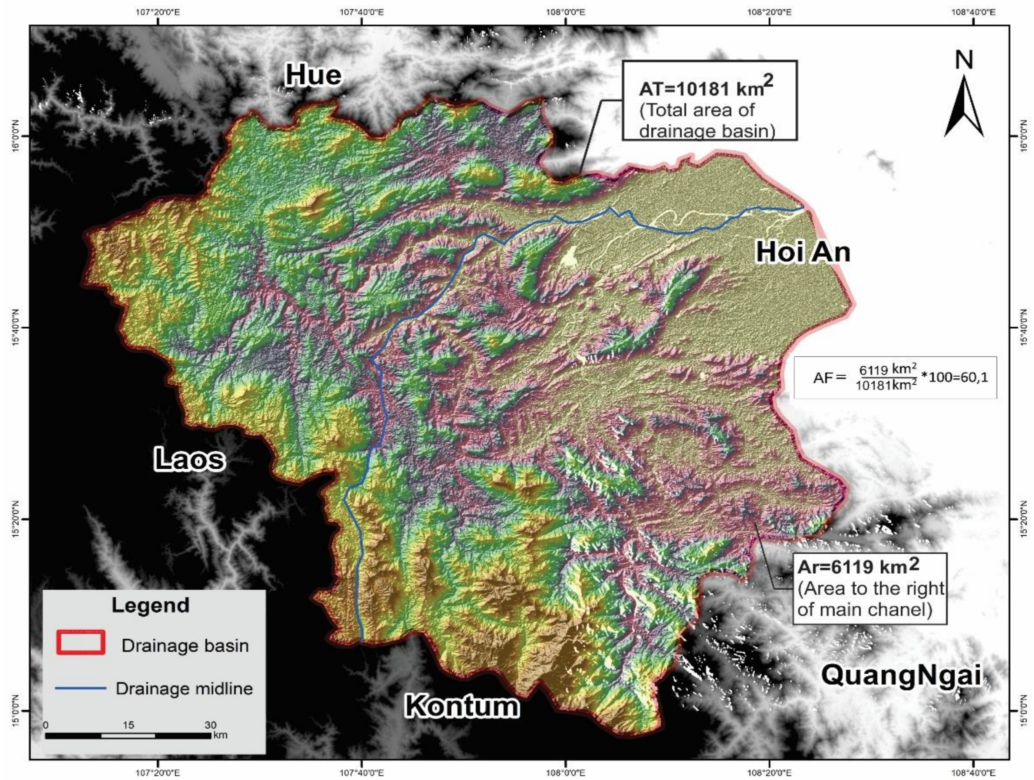

Figure 6. Drainage basin asymmetry (AF = 60.1) of the Quang Nam basin, reflecting a greater subsidence rate on the northern flank (drainage boundary after Luu & von Meding, 2018).

Table 3. Parameters and results of the valley floor width-to-height ratio (Vf) calculation in north-central Vietnam (Eld, Erd - elevations of the left and right divides; Esc - elevation of the valley floor; Vfw - valley floor width).

River	Eld (m)	Erd (m)	Esc (m)	Vfw (m)	Vf	River	Eld (m)	Erd (m)	Esc (m)	Vfw (m)	Vf
R1	520	426.7	53.3	168	0.40		284	276	223	71.2	1.25
	875	1073	477	100	0.20	R14	390	284	27	265	0.85
	624	589	560	26	0.56		514	335	196	130	0.57
R2	883.8	959.1	347	133.9	0.23	R15	278	400	35	561	1.85
	775	700	222	80.4	0.16		223	169	76	122	1.02
	581	437	366	53.6	0.37	R17	469	481	52	191	0.45
	519	533	102	110	0.26		87	91	53	200	5.56
R3	1232.4	1158	502.3	73.0	0.11	R18	253	476	136	134	3.72

River	Eld (m)	Erd (m)	Esc (m)	Vfw (m)	Vf	River	Eld (m)	Erd (m)	Esc (m)	Vfw (m)	Vf
	1178	1154	335	83.3	0.10		125	77	44	211	3.70
R4	1128	1160	860.1	102.6	0.36	R5	768	734	29	90	0.12
	1048	1080	862	30	0.15	R7	273	254	105	97.2	0.61
	95	203	25	40	0.32	H6	146	961	470	30	0.36
H14	430	345	262	20	0.16	H8	547	634	207	45.6	0.12
	338	298	243	28.8	0.38	H7	1027	1189	911	48.5	0.25
R16	233.8	192.9	45.4	66.7	0.40	H9	659	855	440	65.7	0.21
	101	67	29	133	2.42	H10	481	537	233	100	0.36
	170	98	45	147	1.65	H11	515	588	129	76.8	0.18
R12	1060	944	486	177	0.34	R8	1452	1307	908	98	0.21
	680	549	228	233	0.60	R7	1338	1154	880	180	0.49
	326	404	27	300	0.89	R9	874	1002	508	114	0.27
R13	192	212	75	79.8	0.63	R11	1147	955	641	230	0.56
	799	755	428	152	0.44						

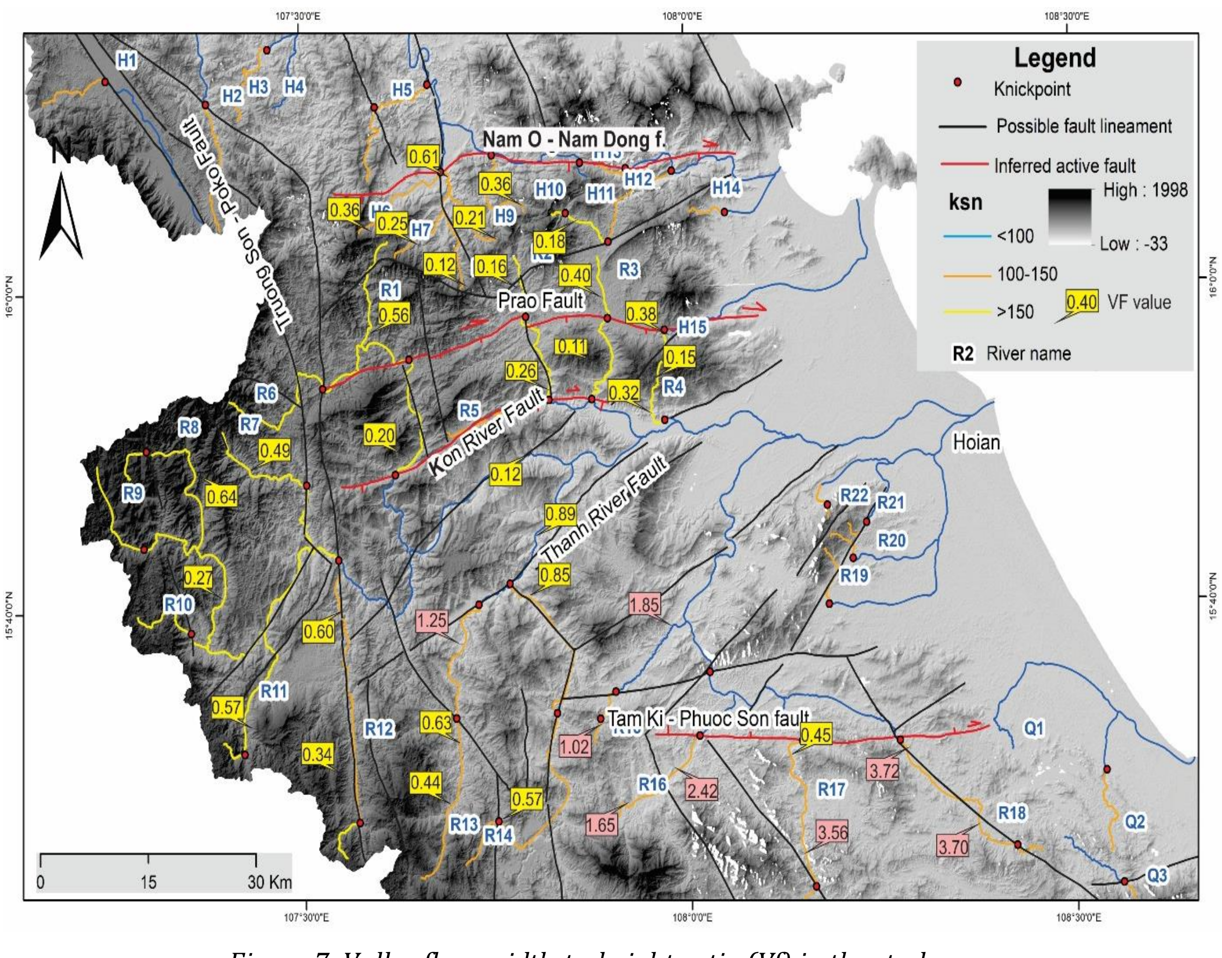

Figure 7. Valley floor width-to-height ratio (Vf) in the study area.

4.5. Field evidence of faulting

Four fault systems were identified from slickenside indicators and fault traces. (I) A pervasive **NE-SW system** (N45°E-N60°E, dipping 50÷60°) shows dextral-normal movement; at outcrop QN1702 a 1-2 m fault scarp offsets the recent surface (Figure 8), and the Dien Ban area forms a hanging-wall depression against uplifted footwalls at Que Son and Dai Loc. (II) A less common **NW-SE system** (S10-20°E) shows right-lateral strike-slip. (III) A near **E-W system** of short normal-sinistral faults forms sharp slopes and triangular facets, well expressed along the Kon River fault at QN1709 (Figure 9). (IV) A locally observed **N-S system** shows normal slickensides.

Figure 8. Outcrop QN1702 (NW Quang Nam) showing the NE-SW fault system with dextral-normal shear-sense indicators; the ~1÷2 m offset of the recent surface indicates an active fault scarp.

5. Discussion

5.1. Tectonic origin of steepness anomalies and knickpoints

Three classes of knickpoint can be distinguished by their setting. Vertical-step knickpoints anchored to erodibility contrasts (R8-R15, R19-R22, Q1-Q3, H1-H5) and dam-induced knickpoints (e.g., H5; Figure 4) lack tectonic significance. By contrast, slope-break knickpoints and elevated k_{sn} (> 150, locally about 300) that occur within uniform lithology and align with mapped faults are best explained by transient incision following fault movement. On this basis, the high-k_{sn} reaches of R1-R5 across the Kon River and Prao faults, the H9-H13 knickpoints along the Nam O-Nam Dong fault, and the R16-R18 anomaly along the Tam Ky-Phuoc Son fault are interpreted as records of recent, reactivated normal faulting rather than lithological or anthropogenic forcing. Consistent with this, channels intersecting the mapped active faults show systematically higher ksn and lower Vf than channels that do not, supporting a tectonic rather than a purely lithological control; a fuller statistical treatment is nonetheless limited by the sample size and the absence of independent slip-rate data.

5.2. Differential subsidence and northward basin tilting

Several independent lines of evidence converge on a greater subsidence rate along the northern flank of the basin. The basin asymmetry (AF = 60.1) records northward displacement of the drainage midline; the valley floor width-to-height ratio is systematically lower on the northern flank

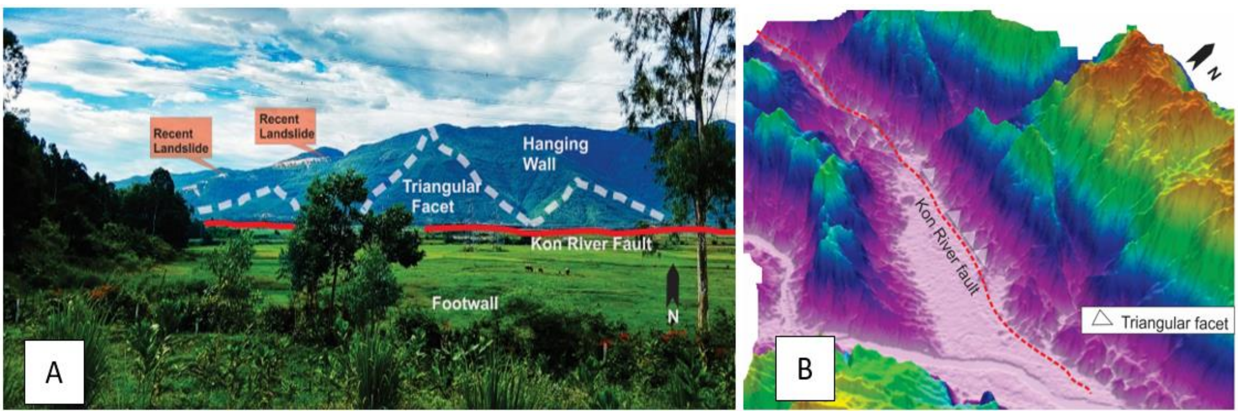

Figure 9. A) Landform indicators of normal movement along the near-E-W Kon River fault at QN1709: fault trace, triangular facets, flat alluvial footwall and high-relief hanging wall. B) Kon River fault trace and triangular facets on a 3-D DEM image.

(0.11÷0.61) than on the southern flank (0.40÷3.72); and swath profiles A1-A2 reveal step-down terrains bounded by the high-angle Prao and Kon River normal faults. Taken together, these indices indicate active northward tilting accommodated by the bounding normal faults, with the highest k_{sn} of the study area at Dai Loc marking the most rapidly responding sector. The convergence of asymmetry, valley-form and channel-steepness signals - rather than any single index - indicates that the Quang Nam landscape is in a transient state of adjustment driven by fault-controlled, base-level lowering.

5.3. Distribution and significance of the active faults

Synthesising the channel, valley and field data, four reactivated normal faults are identified as active: the Nam O-Nam Dong, Prao and Kon River faults to the north and the Tam Ky-Phuoc Son fault to the south (Figure 10; Table 4).

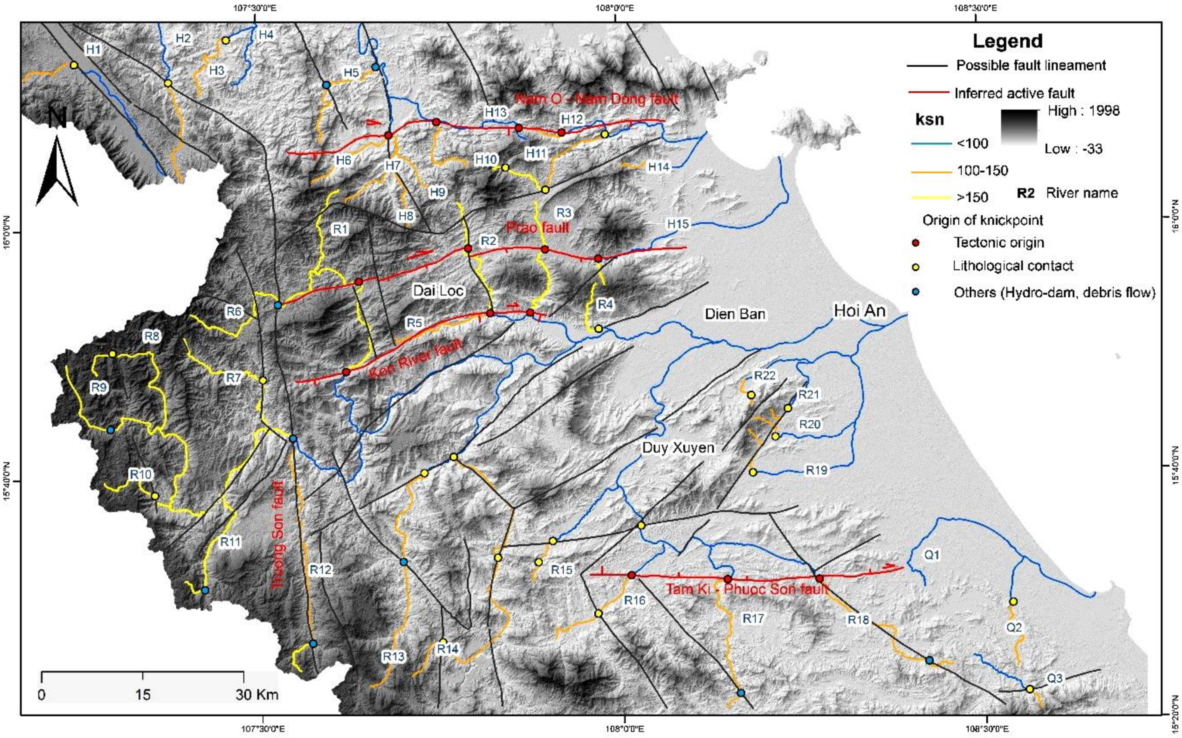

Figure 10. Distribution map of the inferred active faults in the study area.

Table 4. Inferred active faults in the study area, with kinematic and geometric characteristics determined in this study.

Inferred active fault	Localities	Active length (km)	Attitude (dip dir./dip°)	Lithologies of fault walls	Recent shear sense
Nam O-Nam Dong	N of Da Nang (E) to Dong Giang (W)	57	160 / 65	Devonian (Tan Lam Fm.)	Dextral-normal (reactivated)
Prao	N Dai Loc (E) to Tay Giang (W)	63	180 / 55	Cambrian-Ordovician (A Vuong Fm.)	Normal (reactivated)
Kon River	Dien Ban (E) to western area	39	140 / 70	Triassic (Nong Son Fm.)	Normal (reactivated)
Tam Ky-Phuoc Son	Hoi An (E) to Phuoc Son (W)	46	10 / 55	Late Proterozoic (Kham Duc complex)	Normal (reactivated)

Where these faults cross rivers they generate slope-break knickpoints and very high ksn, and their normal slip produces topographic steps and narrow, high-Vf footwall valleys, most clearly on the northern flank. The remaining mapped faults lack a comparable geomorphic and field signature and are not considered demonstrably active. Because horizontal offset cannot be resolved from river profiles, active strike-slip structures (e.g., along the Truong Son fault) may remain undetected and warrant dedicated investigation.

5.4. Tectonic mechanism and hazard implications

The active NE-SW to E-W normal faults, with a sub-horizontal N-S minimum principal stress, are consistent with the changing paleostress field documented from the late Miocene to the present (Vuong & Hoai, 2019) and are interpreted as a far-field response to the ongoing India-Eurasia collision, with the Indian plate moving north-east at about 5 cm yr^{-1} (Hall, 2002; Phan et al., 2013). They provide geomorphic evidence for Holocene fault movement in central Vietnam (Figure 11). The inferred active faults may contribute to recent geohazards, including earthquakes, landslides and ground subsidence leading to coastal erosion and marine incursion; the subsidence rate of about 0.96 mm yr^{-1} reported for the coastal zone (Tran et al., 2015) is consistent with our results. Tectonic subsidence on these normal faults, together with natural compaction and groundwater extraction, therefore plays an important role in enhancing coastal geohazards in the region, with direct implications for hazard assessment under rising sea levels. In the absence of direct geodetic measurements this contribution is inferred rather than measured, and the reported coastal subsidence rate (Tran et al., 2015) is cited only as being consistent with our results. Several limitations should be acknowledged: geomorphic indices can also respond to lithological and climatic variability; the DEM resolution restricts detection of small offsets; and the timing of fault movement is not constrained by dating or geodesy. The tectonic interpretation is therefore preferred only where lithology is uniform and multiple independent indices converge.

6. Conclusions

Field observations and newly extracted geomorphic indices reveal a comprehensive relationship between active tectonics and geohazards in the Quang Nam area, using landform deformation as a marker of recent fault activity concealed by surface processes. The main findings are as follows. (1) The normalised steepness index (k_{sn}) is higher on channels intersecting the NE-SW to E-W faults (Nam O-Nam Dong, Prao, Kon River and

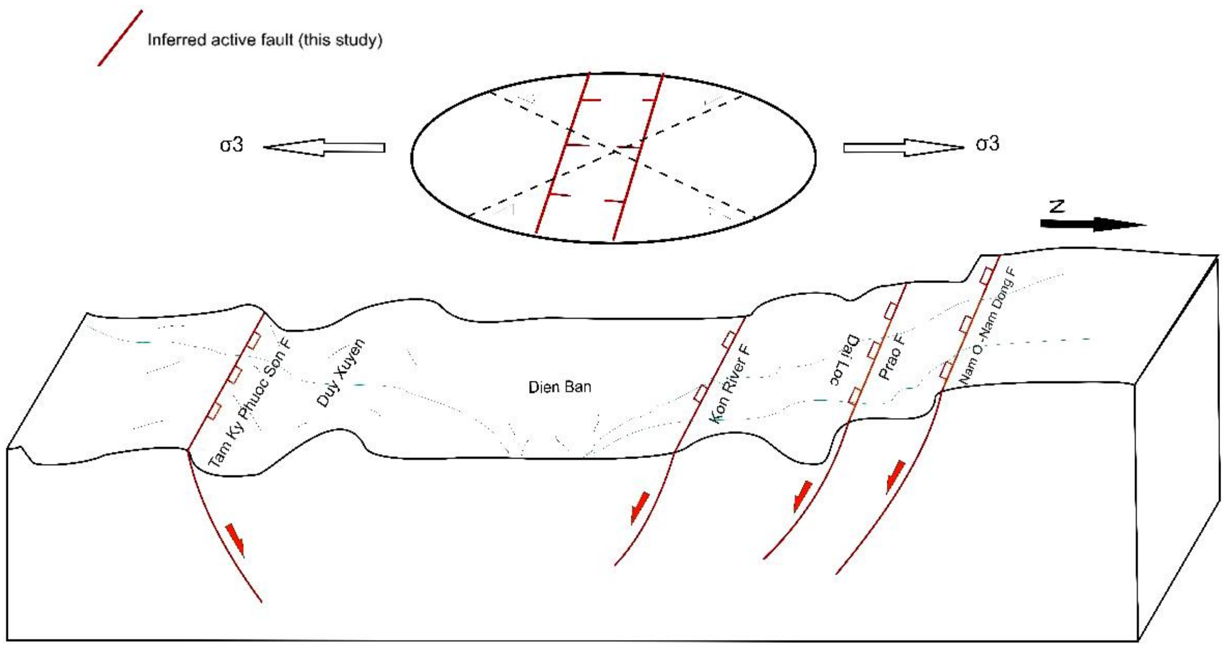

Figure 11. Conceptual model of the relationship between active faulting and subsidence in the Quang Nam area.

Tam Ky-Phuoc Son), which are confirmed as active normal faults by field slickenside indicators. (2) The drainage basin asymmetry (AF = 60.1) shows northward tilting of the basin, reflecting lithological heterogeneity and the influence of active tectonics. (3) The valley floor width-to-height ratio is lower on the northern flank (0.11÷0.61) than on the southern flank (0.40÷3.72), indicating differential subsidence/uplift. (4) The NE-SW to E-W faults, with a sub-horizontal N-S minimum principal stress, may drive tectonic subsidence in the Quang Nam area and threaten its inhabitants. Future work should focus on dating fault movement and on geophysical detection of horizontal displacement to fully constrain the recent stress regime.

Acknowledgements

This study was supported by Hanoi University of Mining and Geology under grant number T26-14.

Contributions of authors

Vu Anh Dao - conceived the study, processed the DEM and geomorphic indices, carried out the fieldwork, analysed the data and wrote the manuscript; Tran Thanh Hai, Bui Vinh Hau, Ngo Thi Kim Chi - supervised the research, contributed to the methodology and interpretation, and revised the manuscript; Phan Van Binh, Nguyen Quoc Hung - contributed to the geomorphic analysis and reviewed the manuscript. All authors approved the final version.

References

Bull, W. B., & McFadden, L. D. (1977). Tectonic geomorphology north and south of the Garlock fault, California. In D. O. Doehring (Ed.), *Geomorphology in arid regions* (pp. 115-137). Routledge.

Burbank, D. W., & Anderson, R. S. (2011). Tectonic geomorphology (2nd ed.). Wiley-Blackwell.

Di Naccio, D., Boncio, P., Brozzetti, F., Pazzaglia, F. J., & Lavecchia, G. (2013). Morphotectonic analysis of the Lunigiana and Garfagnana grabens (northern Apennines, Italy): Implications for active normal faulting. *Geomorphology*, 201, 293-311. https://doi. org/10.1016/j.geomorph. 2013.07.003.

Dinh, T. H., Chan, Y. C., & Chang, C. P. (2021). Deformation patterns and potential active movements of the Fansipan mountain range, northern Vietnam. *International Journal of Earth Sciences*, 110(1), 35-51. https://doi.org/ 10.1007/s00531-020-01934-5.

Faure, M., Lepvrier, C., & Nguyen, V. V. (2014). The South China block-Indochina collision: Where, when, and how? *Journal of Asian Earth Sciences*, 79, 260-274. https://doi.org/10. 1016/j.jseaes.2013.09.022.

Hall, R. (2002). Cenozoic geological and plate tectonic evolution of SE Asia and the SW Pacific: Computer-based reconstructions, model and animations. *Journal of Asian Earth Sciences,* 20(4), 353-431. https://doi.org/10. 1016/ S1367-9120(01)00069-4.

Hieu, P. T., Dung, N. T., Thuy, N. T. B., Minh, N. T., & Minh, P. (2016). U-Pb ages and Hf isotopic composition of zircon and bulk rock geochemistry of the Dai Loc granitoid complex in Kontum massif: Implications for early Paleozoic crustal evolution in central Vietnam. *Journal of Mineralogical and Petrological Sciences*, 111(5), 326-336. https://doi.org/10. 2465/jmps.151022.

Huchon, P., Le Pichon, X., & Rangin, C. (1994). Indochina Peninsula and the collision between India and Eurasia. *Geology*, 22(1), 27-30.

Hutchison, C. S. (1989). Geological evolution of South-East Asia. Oxford University Press.

Keller, E. A., & Pinter, N. (2002). Active tectonics: Earthquakes, uplift, and landscape (2nd ed.). *Prentice Hall.*

Kirby, E., & Ouimet, W. (2011). Tectonic geomorphology along the eastern margin of Tibet: Insights into the pattern and processes of active deformation adjacent to the Sichuan Basin. *Geological Society, London, Special Publications*, 353(1), 165-188. https://doi. org/ 10.1144/SP353.9.

Kirby, E., & Whipple, K. X. (2012). Expression of active tectonics in erosional landscapes. *Journal of Structural Geology*, 44, 54-75. https://doi. org/10.1016/j.jsg.2012.07.009.

Lan, C. Y., Chung, S. L., Long, T. V., Lo, C. H., Lee, T. Y., Mertzman, S. A., & Shen, J. J. S. (2003). Geochemical and Sr-Nd isotopic constraints from the Kontum massif, central Vietnam, on the crustal evolution of the Indochina block. *Precambrian Research*, 122(1-4), 7-27.

Leeder, M. R., & Jackson, J. A. (1993). The interaction between normal faulting and drainage in active extensional basins, with examples from the western United States and central Greece. *Basin Research*, 5(2), 79-102.

Lepvrier, C., Maluski, H., Nguyen, V. V., Roques, D., Axente, V., & Rangin, C. (1997). Indosinian NW-trending shear zones within the Truong Son belt (Vietnam): 40Ar-39Ar Triassic ages and Cretaceous to Cenozoic overprints. *Tectonophysics*, 283(1-4), 105-127.

Lepvrier, C., Maluski, H., Vu, V. T., Leyreloup, A., Phan, T. T., & Nguyen, V. V. (2004). The Early Triassic Indosinian orogeny in Vietnam (Truong Son belt and Kontum massif): Implications for the geodynamic evolution of Indochina. *Tectonophysics*, 393(1-4), 87-118.

Li, S., Advokaat, E. L., van Hinsbergen, D. J. J., Koymans, M., Deng, C., & Zhu, R. (2017). Paleomagnetic constraints on the Mesozoic-Cenozoic paleolatitudinal and rotational history of Indochina and South China: Review and updated kinematic reconstruction. *Earth-Science Reviews*, 171, 58-77. https://doi.org/10.1016/j.earscirev.2017.05.007.

Luu, C., & von Meding, J. (2018). A flood risk assessment of Quang Nam, Vietnam, using spatial multicriteria decision analysis. *Water*, 10(4), 461. https://doi.org/10.3390/w10040461.

Mahmood, S. A., & Gloaguen, R. (2012). Appraisal of active tectonics in Hindu Kush: Insights from DEM-derived geomorphic indices and drainage analysis. *Geoscience Frontiers*, 3(4), 407-428.

Mukherjee, S., & Joshi, P. K. (2013). Evaluation of vertical accuracy of open-source Digital Elevation Model (DEM). *International Journal of Applied Earth Observation and Geoinformation*, 21, 205-217.

Nguyen, V. T. (Ed.). (1986). Geological map of Vietnam at 1:200,000 scale, Thua Thien Hue-Quang Ngai sheets. *Geological Survey of Vietnam.*

Ozkaymak, C., & Sozbilir, H. (2012). Tectonic geomorphology of the Spildagi high ranges, western Anatolia. *Geomorphology*, 173-174, 128-140.

Pérez-Peña, J. V., Azor, A., Azañón, J. M., & Keller, E. A. (2010). Active tectonics in the Sierra Nevada (Betic Cordillera, SE Spain): Insights from geomorphic indices and drainage pattern analysis. *Geomorphology*, 119(1-2), 74-87.

Pérez-Peña, J. V., Al-Awabdeh, M., Azañón, J. M., Galve, J. P., Booth-Rea, G., & Notti, D. (2017). SwathProfiler and NProfiler: Two new ArcGIS add-ins for the automatic extraction of swath and normalized river profiles. *Computers & Geosciences*, 104, 135-150. https://doi.org/10.1016/j.cageo.2016.08.008.

Phan, T. T., Hoang, Q. V., Nguyen, V. H., & Ngo, V. L. (2013). Active fault segmentation and seismic hazard in Hoa Binh reservoir, Vietnam. *Central European Journal of Geosciences*, 5(2), 223-235.

Santillan, J. R., & Makinano-Santillan, M. (2016). Vertical accuracy assessment of 30-m resolution ALOS, ASTER, and SRTM global DEMs over north-eastern Mindanao, Philippines. International Archives of the Photogrammetry, *Remote Sensing and Spatial Information Sciences*, 41(B4), 149-156.

Sone, M., & Metcalfe, I. (2008). Parallel Tethyan sutures in mainland Southeast Asia: New insights for Palaeo-Tethys closure. *Comptes Rendus Geoscience*, 340(2-3), 166-179.

Tapponnier, P., Peltzer, G., Le Dain, A. Y., Armijo, R., & Cobbold, P. (1982). Propagating extrusion tectonics in Asia: New insights from simple experiments with plasticine. *Geology*, 10(12), 611-616.

Tran, H. T., et al. (2013). The Tam Ky-Phuoc Son shear zone in central Vietnam: Tectonic and metallogenic implications. *Gondwana Research,* 26(1), 144-164.

Tran, T. H., Phi, T. P. T., Le, H. M., Vu, D. A., Bui, M. T., Nguyen, N. X., & Hoang, T. D. N. (2015). The role of active tectonic movement on coastal geological hazards: A case study of central Vietnam's coastal zone. *In Proceedings of the International Conference on Geology, Geotechnology and Mineral Resources of Indochina (GEOINDO 2015)* (pp. 1-12). Khon Kaen, Thailand.

Tri, T. V., & Khuc, V. (Eds.). (2011). Geology and earth resources of Vietnam. *Publishing House for Science and Technology.*

Usuki, T., Lan, C. Y., Yui, T. F., Iizuka, Y., Vu, V. T., Tran, T. A., & Okamoto, K. (2009). Early Paleozoic medium-pressure metamorphism in central Vietnam: Evidence from SHRIMP U-Pb zircon ages. *Geosciences Journal*, 13(3), 245-256.

Vuong, N. V., & Hoai, L. T. T. (2019). Cenozoic paleostress evolution in south-central Vietnam: Implication for changing dynamics of faulting along the eastern Indochina continental margin. *Journal of Asian Earth Sciences,* 185, 104006. https://doi.org/10.1016/j.jseaes.2019.104006.

Whipple, K. X. (2004). Bedrock rivers and the geomorphology of active orogens. *Annual Review of Earth and Planetary Sciences*, 32, 151-185.

Whipple, K., Wobus, C., Crosby, B., Kirby, E., & Sheehan, D. (2007). New tools for quantitative geomorphology: Extraction and interpretation of stream profiles from digital topographic data [GSA short course*]. Geological Society of America.*

Wobus, C., Whipple, K. X., Kirby, E., Snyder, N., Johnson, J., Spyropolou, K., Crosby, B., & Sheehan, D. (2006). Tectonics from topography: Procedures, promise, and pitfalls. In S. D. Willett, N. Hovius, M. T. Brandon, & D. M. Fisher (Eds.), Tectonics, climate, and landscape evolution (GSA Special Paper 398, pp. 55-74). *Geological Society of America*. https://doi.org/10.1130/ 2006.2398(04).